Journal of Civil Engineering (IEB), 33 (2) (2005) 91-103

Journal of
Civil Engineering
IEB

A study on reinforced concrete skew slab behavior

Md. Khasro Miah[1] and Ahsanul Kabir[2]

[1] *Department of Civil Engineering*
Dhaka University of Engineering and Technology, Gazipur 1700, Bangladesh
[2]*Department of Civil Engineering*
Bangladesh University of Engineering and Technology, Dhaka 1000, Bangladesh

Received on 06 December 2005

Abstract

The behaviour of reinforced concrete skew slabs under vertical concentrated loads is reported in this paper. A total of six slabs were tested in the Concrete Laboratory of Bangladesh University of Engineering and Technology (BUET), Dhaka. All the test slabs were $1/6^{th}$ scale models of prototype skew slabs having opposite edges simply supported. The same steel arrangement was used for all the slabs. Main steel was parallel to free edges and distribution steel was parallel to support line. Two aspect ratio viz., 0.85 and 1.50 were selected for the study. Centrally located single concentrated load and four point loads equally spaced across the mid-span were the two types of loading condition studied. Two different skew angles viz., $\alpha = 25°$ and 45° were the other parameters of study. The experimental observations were limited to measurement of deflection at different nodal points, concrete fiber strains at some top and bottom points of the slabs, steel strains, cracking patterns and observing the cracking and ultimate loads. Numerical analysis was also carried out for the test slabs to verify the experimental results.

© 2005 Institution of Engineers, Bangladesh. All rights reserved.

Keywords: Reinforced Concrete, Skew Slab, Point Loads, Aspect ratio, Cracking Load, Ultimate Load, Crack Pattern..

1. Introduction

Skew slab can be defined as a four-sided slab having equal opposite angles other than 90°. Skew angle (α) is usually measured clockwise from the vertical line perpendicular to the support line of the skew slab. Aspect ratio (r) is defined as the ratio of span to width of the supports. Due to skewness of the structure, the stress and deflection characteristics are quite different from those observed in right bridge deck slabs. Laboratory test facility dictated that a ne-sixth scale model be selected which was also found be adequate from dimensional analysis of the model with respect to the prototype.

The constitutive relation of the model materials was geometrically similar to the one of the prototype, which is important for taking into account the material similitude [Zia et al. (1970)]. For the purpose of geometric similitude between the prototype and the model, all the linear dimensions of the model were scaled down from the corresponding dimensions of the prototype by a constant ratio. The concentrated load was applied on the model through a 15mm thick hard rubber pad underneath a steel plate to spread the load over an area of 50mm square. This was done to approximate the tyre effect of the vehicles wheel on prototype.

Reinforced concrete skew slabs are widely used in bridge construction when the roads cross the streams and canals at angles other than 90 degrees. They are also used in floor system of reinforced concrete building as well as load bearing brick buildings where the floors and roofs are skewed for architectural reasons or space limitations.

Due to increasing population in Bangladesh, the demand for more roads and highways are increasing and more of them would require more intersections of roads and highways. To maintain steady flow of traffic in these intersections it will be necessary that they be designed with grade separation, which indicates that more skew slab and deck bridges will be constructed in future. This investigation is an attempt to study the physical behaviour of skew slabs more closely and delineate the response observed. The experimental observation like deflection and ultimate loads are compared with numerical results obtained using layered finite element formulation [Doullah and Kabir (1997)].

2. Review of previous work

A number of researchers have investigated experimentally the behaviour of skew reinforced concrete slabs. Islam (1996) investigated the behaviour of reinforced concrete skew slabs designed for axle loading and self-loads at service condition. Experimental investigation was carried out on 30 degrees skew slab with an aspect ratio of two-third. The right span was 16 ft and right width was 24 ft. Four skew slabs were tested. Two of the test slabs had main reinforcement parallel to free edge and the other two had them laid orthogonal to the support. Distribution reinforcement was parallel to the supports for all the four slabs. His primary interest were observation of vertical deflections along centre lines parallel to the supports and free edges at self load and service load, crack pattern and concrete strain at some pre-selected location on concrete surface.

Jahan (1989) investigated eight slabs with skew angles 0°, 15°, 30° and 45°. Four of them with edge beams and remaining four without edge beams. The right span was 15 ft and right width 22.5 ft making the aspect ratio of 0.67. All dimension including reinforcements of models were scaled down to one-sixth of the prototype. Steel arrangements for main reinforcement were perpendicular to support and distribution reinforcement parallel to support. The investigation records were deflection at central point and variation of longitudinal and transverse deflections along central lines parallel to free edges and parallel to supports. He also compared the experimental results with the theoretical results and studied the effect of cyclic loading on load-deflection response.

El-hafez (1986) investigated six skew slabs with skew angles 30°, -30° and 45°. There were four slabs with skew angle 45°, one of them was ribbed skew slab. The right span of all the slabs was 2100 mm but support length was 1945 mm for 30° and -30° skew angle slabs and 2000 mm for 45° skew angle slabs. The main reinforcement was parallel

to free edge and transverse reinforcement parallel to support for skew angles 30° and -30°. But reinforcement arrangement for the four slabs with skew angle 45° was different from one another. Experimental observations of her investigation were deflections normal to the plane of the slab, strains on concrete surfaces, steel strains and crack pattern. In fact the primary aim of her experimental investigation was to validate the direct design method for skew slabs using finite element analysis.

Cope and Rao(1983) investigated the behaviour of reinforced concrete skew slab bridges, designed for AASHTO (1983) HS Truck loading, at service and ultimate stage. Linear elastic theory of plate analysis was used. Experimental investigation was carried out on 45° skew reinforced concrete slab bridge model with aspect ratio of 1.0. One of the models was reinforced perpendicular and parallel to support and the other was reinforced perpendicular and parallel to free edge. The slabs were tested for AASHTO HS truck loading and deflection and surface strains were recorded.

Desayi and Probhakara (1981) investigated skew slabs restrained at all edges to study the load-deflection behaviour at ultimate load condition for yield line analysis. Slabs with skew angles 15°, 30° and 45° having aspect ratio of 1.50 were tested. The slabs were subject to uniformly distributed loading simulated by sixteen point loads. Central and quarter point deflections were observed. Analytical results were comparable to the experimental findings with slight over-estimated deflection, but better agreement was observed between experimental and computed ultimate load.

3. Finite element formulation

An eight-noded isoperimetric Mindlin plate element (Fig. 1 and 2) using layered representation across the thickness has been employed to get the numerical solution of the skew slabs having the different aspect ratios and skew angles. In the layered approach reinforced concrete plate is assumed to be composed of layers of concrete and steel (Fig. 3), each of which lying in a state of plane stress. This permits stresses to vary across the plate thickness considering piecewise constant approximation. Each node contains five degrees of freedom, two membrane displacements u and v, one lateral displacement w, and two independent rotations θx, θy. The layer in-plane displacements u and v are related to nodal degree of freedom through standard transformation. The incremental stress-strain relation may be expressed as

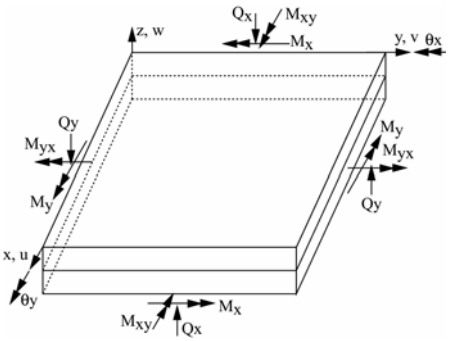

Fig. 1. Typical Mindlin plate element with sign convention

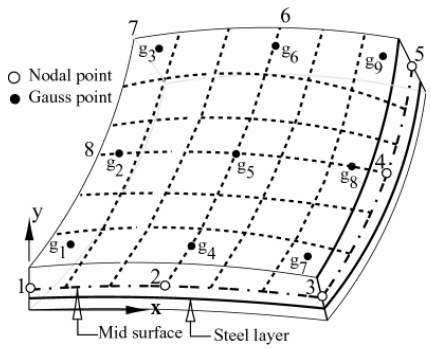

Fig. 2. Eight noded isoparametric plate bending element

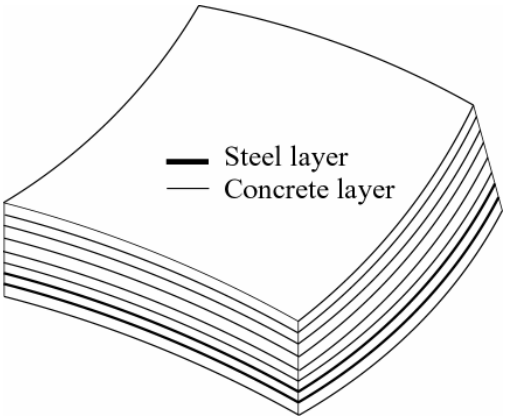

Fig. 3. Layered element

$$\underline{\varepsilon}_p = \sum \underline{B}_{pi}\underline{d}_i \text{ and } \underline{\varepsilon}_s = \sum \underline{B}_{si}\underline{d}_i \tag{1}$$

where,

$\underline{B}_{pi}$ = Strain matrix due to plane stress deformation

$\underline{B}_{si}$ = Strain matrix due to plane transverse shear deformation

The following are the incremental stress-strain relationships

$$\Delta\underline{\sigma}_p = \underline{D}_p\Delta\underline{\varepsilon}_p \text{ and } \Delta\underline{\sigma}_s = \underline{D}_s\Delta\underline{\varepsilon}_s \tag{2}$$

where,

$\underline{D}_p$ = Elasticity matrix related to in-plane stresses

$\underline{D}_s$ = Elasticity matrix related to transverse shear stresses

Finally, the stiffness matrix and the load vectors are obtained from the following expressions

$$\left.\begin{aligned} K_{ij} &= \int_V \underline{B}_{pi}{}^T \underline{D}_p \underline{B}_{pj} dV + \int_V \underline{B}_{si}{}^T \underline{D}_s \underline{B}_{sj} dV \\ f_i &= \int_V \underline{N}_i{}^T \underline{b} dV \end{aligned}\right\} \tag{3}$$

where, $\underline{b}$ = body force

3.1 Constitutive relations

Reinforced concrete is a composite of concrete and steel. The primary non-linearity at very early stage of loading is introduced due to cracking of concrete. At the later stage, the stress-strain nonlinearity is exhibited both in concrete and steel. The details of non-linear constitutive relations used for concrete and steel is described elsewhere [Doullah and Kabir (1997), Doullah (2000)].

4. Experimental investigations

Six model skew slabs have been experimentally tested in the Concrete Laboratory of BUET. These investigations have been carried out to study the behaviour of reinforced concrete skew slabs subject to point load/s (2000). The test slabs are designated as slab S1 through slab S6 depending upon aspect ratio and types of loading. Slabs S1, S2 and S5 were tested with centrally located single concentrated load and the rest were tested with four point loads placed at equal interval on the centre span. The six slabs tested may be grouped into three groups depending on their aspect ratios and skew angles. The grouping is summarized in Table 1. The span length, defined as support to support perpendicular distance was 1200 mm and the slab thickness was 75 mm for all the test slabs.

4.1.1 Casting of slabs

The test slabs were cast using Ordinary Portland Cement (ASTM Type-1), Sylhet sand (F. M. = 2.85) as fine aggregate and stone chips [3/4" (20-mm) down graded] as coarse aggregate. The aggregate gradation conforms to the requirements of ASTM C136-88 recommendations [ASTM (1988)]. The flexural reinforcements used in the test slabs were 40 grade 10 mm deformed bar. The physical properties viz. actual diameter, yield strength, ultimate strength and percentage elongation of reinforcing bars used are 8.40mm, 280 MPa, 465 MPa and 26.7%, respectively.

Table 1
Test Slab Grouping

Group No.	Slab Designation	Slab Dimension (mm x mm)	Skew Angle (α)	Aspect Ratio (r)	Loading Type
1.	S1	1412 x 1200	45°	0.85	Single point
	S3	1412 x 1200	45°	0.85	Four points
2.	S2	1412 x 1200	25°	0.85	Single point
	S4	1412 x 1200	25°	0.85	Four points
3.	S5	800 x 1200	25°	1.50	Single point
	S6	800 x 1200	25°	1.50	Four points

The water cement ratio of concrete mix was 0.50 and the concrete mix ratio was 1: 2.30: 2.65 (by weight) of Cement : Sand : Stone Chips. The form works for the test slabs were made of steel plate and boundaries formed with steel angles. The boundary angles were either welded or fastened with nut and bolts to make the desired skew slab dimensions. The boundary frame was supported on steel plate, which rested over a timber frame. Finally, the timber frame rested on the floor of the laboratory.

Steel reinforcement was calculated for 7.2 m span prototype slab subject to standard AASHTO H20 truck loading. Steel for the 1.2 m span models were then appropriately scaled down. On completion of the reinforcement assembly, some electric strain gauges (TML, type FLA-5-11) and terminals (TML, type TFY-2S) were installed on the main and transverse bars at some selected locations close to some Gaussian integration points of finite elements used for numerical solution. The Gauss point coordinates were computed using a finite element program developed by Doullah (2000) based on eight-

noded isoparametric Mindlin layered plate element formulation (Fig. 1, 2 and 3). The element discretisation, boundary conditions, loading types and locations of point loads employed for the finite element analysis of a typical slab is shown in Fig. 4. Typical reinforcement layout with the strain gauge locations in steel as well as deflection recording stations of the Slab S1 is given in Fig. 5.

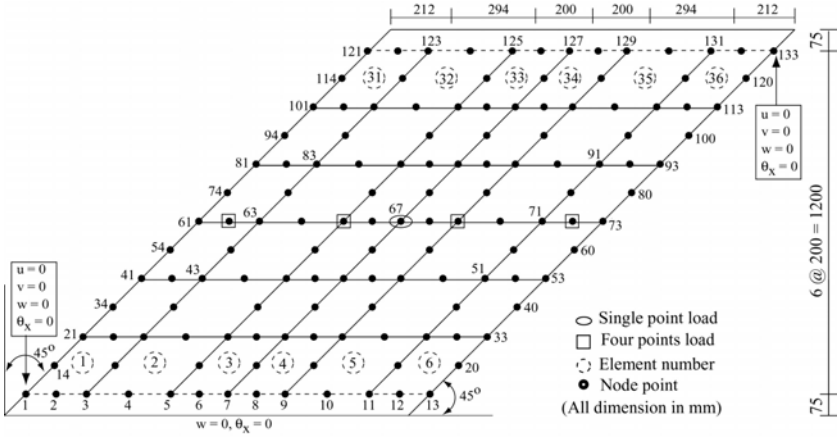

Fig. 4. Element discretisation for slabs
S1 and S3 with necessary boundary conditions

The reinforcement assembly with the installed strain gauges was placed on the base of the prepared formwork for the respective model. Mortar blocks 12 mm thick were used between the form base and the reinforcement to maintain desired clear cover. The slab models were cast in the concrete laboratory. The formwork for casting was placed on the floor of the laboratory with proper arrangement. Lubricating oil was used to smear the bottom and side of the shutter for its easy removal after hardening of the concrete. The reinforcement mesh was then properly positioned inside the formwork. Fresh concrete was prepared as per designed mix in a drum type mixture machine. Immediately after unloading from mixture machine, the fresh concrete was placed in the form and compacted by using nozzle type vibrator. The top surface was leveled using a wooden float. A total of six cylinders of standard size were cast simultaneously as a control specimen for determining the compressive and tensile strength of slab concrete.

Before fixing of Electrical Strain Gauges on the concrete surfaces, the test slabs were white washed on either faces using a solution of lime in water. About three to four coats of white wash were applied. Each coat was applied after drying of the previous coat of white wash. The Electric Strain Gauges (TML, type PL-60-11) were fixed both at top and bottom surface of the test slabs at some pre-selected locations after proper cleaning of the spots with sand paper.

4.2 Testing of Slabs

Six reinforced concrete skew slabs were tested, each of which was loaded with either single concentrated load or four concentrated loads as summarized in Table 1. All the slabs were simply supported on two opposite edges. The test slab was placed on its supports. After checking for any possible damage, all the electrical strain gauges were connected to the data logger through a scanner junction box. The deflection transducers were placed at their proper grid point locations for recording deflections and checked to

ensure that they were vertical and they would operate properly during the test. After all the primary checks, initial zero load readings for the load cell, deflection dial gauges and strain gauges were taken. The test was then continued applying the load at suitable increments, so as to reach the ultimate load in about twenty-five installments. Loading arrangement for the application of four point loads is shown in Fig. 6.

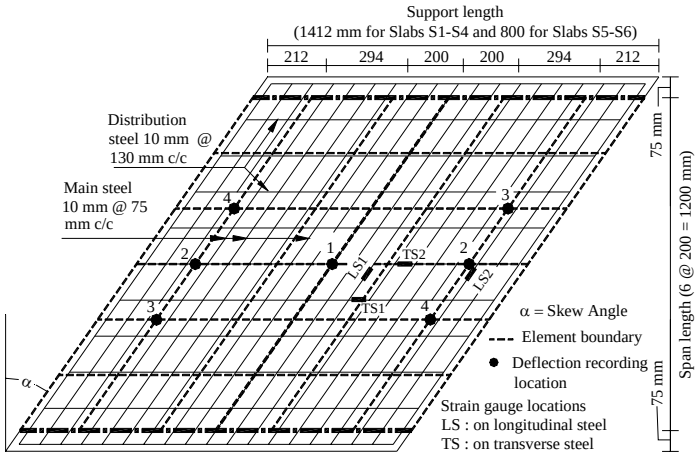

Fig. 5 Typical reinforcement layout with deflection recording stations and locations of Strain gauges in Slab S1

The readings of the load cell, deflection transducers and electrical strain gauges were simultaneously read and printed out at 250 kg (2.5 kN) interval as indicated by dial reading of the testing machine. However, the actual load was recorded as indicated by the load transducers fitted to the machine. The process was repeated until the failure load was reached. The ultimate stage was assumed to have been reached when the deflection readings continuously moved on without any significant change in the applied load. The crack widths of some of the prominent cracks were measured at failure. An optical crack measuring device was used for such measurements with accuracy of up to 0.02 mm

At the end of every slab test, the accompanying cylinders cast as control specimens were tested to assess the compressive and tensile strengths of concrete respectively. Three cylinders were tested for compression and three for split tensile strength and their respective average value was considered as the representative value of slab concrete strengths. The average test results of the control cylinder specimens are summarized in Table 2 for the test slabs.

Table 2
Result of Control Cylinder Specimens

Slab designation	Average crushing strength (MPa)	Average split tensile strength (MPa)
S1, S2	26.5	3.0
S3, S4	28.5	3.0
S5	22.8	2.5
S6	29.4	3.1

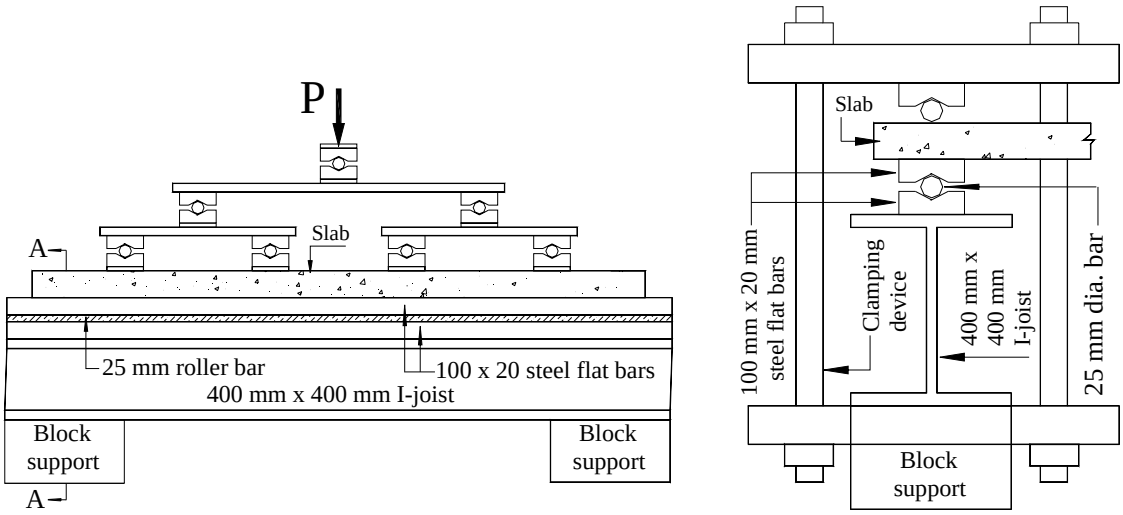

Fig. 6. Details of four points loading arrangement

.

5. Observation and discussion on test results

Some basic behavioural observations of the test slabs as noticed and recorded during the experimental investigations are briefly discussed and presented in the following articles.

5.1 Deflection

The deflections were measured at some selected location for all the test slabs with the help of deflection transducers. The load-deflection response at the central point of all the test slabs for the entire loading history up to failure is shown in Fig. 7 along with the results obtained from finite element analysis. The numerical results agree reasonably with the experimental results for the test slabs. This includes slabs supporting both single point load and four point loads. As expected, the deflection recorded at central nodal point is found to be more in slabs having higher skew angles (45°) compared to the slabs with lower skew angles (25°). Slab thickness remaining constant, stiffness of skew slabs decrease with increase in skew angle. Comparing the two types of loading, it was observed that skew slabs supporting four point loads across the mid span deflected less at the centre span than the slabs supporting single point load at centre span. This is expected as the four point loads are some what distributed over a central band line compared to the single point load at the centre, thus reducing the point deflection at the centre. The maximum deflection of slabs S1, S2, S3 and S4 having identical aspect ratio was found to depend on the skew angle and loading types as well. As can be observed from Table 3, the deflections at obtuse zones were found to be more than acute zones in slabs S1, S2, S3 and S4, all having aspect ratios less than unity (i.e. 0.85) but reverse observation is recorded for slabs S5 and S6 having aspect ratio over unity (i.e. 1.5). This indicates that the aspect ratio of skew slabs influences the flexibility of acute and obtuse angled zones.

5.2 Concrete Strains

The top and bottom strains of concrete surface at some pre-selected Gauss point were recorded. From the strain gauge readings fixed on the concrete surface, some general

trends have been observed. It was found that the bottom surface concrete strains have relatively higher values in obtuse zones of skew slabs compared to similar location in the acute zones for slabs having lower aspect ratios (r=0.85 e.g. slabs S1 to S4). On the contrary, bottom surface concrete strains are relatively lower in obtuse zones compared to acute zones for slabs with relatively higher aspect ratios (r = 1.50 e.g. Slabs S5 and S6). Similar response was also noticed for defection as mentioned in the preceding article.

5.3 Cracking Load

The load at the first visible crack termed as cracking load was recorded for each test slab and are furnished in Table 4 along with the numerical cracking load obtained from numerical analysis of the model slabs. For all the test slabs, the numerical cracking load is about 80% of the experimental cracking loads and the correlation coefficient of the ratios is determined as 0.99. Cracks were observed in the test slabs between 20 to 25 percent of the respective ultimate loads. For the same loading condition, the cracking load of the slabs with lower skew angle (α) were higher compared to slabs with higher skew angle. Similarly, under identical loading condition, the cracking load of the slabs with lower aspect ratio (r) was higher compared to the slabs with higher aspect ratio. Numerically obtained cracking load is expected to be lower than the experimental value. This is because the former corresponds to the numerical load that causes the tensile strength to be exceeded at any sampling integration point while the actual is the value when cracking is significant to be visible in naked eye.

Table 3
Deflections at the Obtuse and Acute Zones of Skew Slabs

Slab Designations	Aspect ratio (r)	Load 50% of P_{ult}		Load 75% of P_{ult}	
		Acute zone (location-3) (mm)	Obtuse zone (location-4) (mm)	Acute zone (location-3) (mm)	Obtuse zone (location-4) (mm)
S1	0.85	1.704	2.371	4.148	5.148
S2	0.85	0.735	1.233	1.850	2.418
S3	0.85	1.000	1.915	2.504	3.126
S4	0.85	1.724	2.098	2.560	4.107
S5	1.50	1.538	1.378	2.730	2.356
S6	1.50	1.013	0.880	1.653	1.285

5.4 Ultimate Load Carrying Capacity

The load at failure condition recorded for each test slab is defined as the ultimate load shown in Table 4. Numerical failure load is also listed with the experimental one to compare one with another. The agreements between the experimental and numerical failure loads are quite well can be seen from Table 4. The numerical failure load is less than the experimental one for the slabs with lower aspect ratio. On the other hand, slabs with higher aspect ratio, the numerical and experimental failure loads are almost equal. Similar to the cracking load, the ultimate loads of the slabs with lower skew angle were also higher compared to slabs with higher skew angle for the same loading condition. The ultimate load of the slabs with lower aspect ratio was found to be higher compared to the slabs with higher aspect ratio under identical loading condition.

5.5 Cracking Pattern

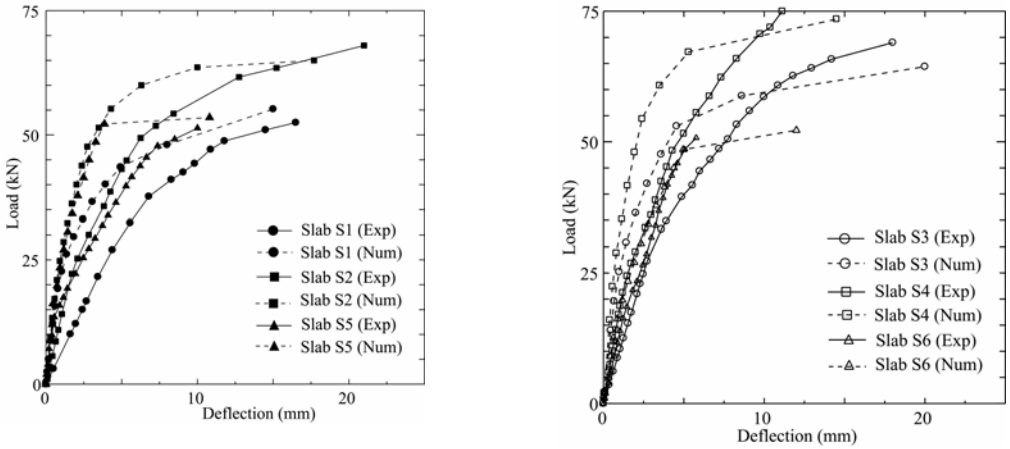

(a) Single Point load (b) Four Point loads

Fig. 7. Load-deflection Diagrams at the centre of all slabs

The cracking patterns of all the test slabs were observed and photograph taken after test. Loading system on the skew slabs appears to have significant influence on the crack patterns. The first crack was always observed at concrete bottom surface near the mid span. For single point loading, a number of cracks originated from the bottom of mid span area and propagated nearly parallel to the support lines towards the free edges like a mesh crack. In case of four-point loading representing a line load, the cracks were limited within a narrow band of centre span. The widths of the major cracks were measured at failure load by an optical crack-measuring device. The cracking patterns at the bottom surface of two test slabs are shown in Fig. 8 and Fig. 9. The crack widths of the prominently visible cracks at failure were measured. Crack width as large as 5 mm was recorded for slabs S3 and S6. In other slabs, crack widths ranged between 1.5 mm to 4 mm at failure. It may be noted that relatively wider cracks were observed in case of four-point loading representing knife-edge loading.

Table 4
Cracking and Failure Loads for the Test Slabs

Slab designation and size (mm x mm)	Types of loading	Skew angle (α)	Experimental cracking load, P_{cr} (kN)	Numerical cracking load, $P_{cr(n)}$ (kN)	$\frac{P_{cr(n)}}{P_{cr}}$	Experimental failure load, P_{expt} (kN)	Numerical failure load, $P_{ult(n)}$ (kN)	$\frac{P_{ult(n)}}{P_{expt}}$
S1 1412 x 1200	One point	45° (r=0.85)	10.50	8.50	0.80	52.50	50.00	0.95
S2 1412 x 1200	One point	25° (r=0.85)	12.40	9.25	0.75	68.00	65.00	0.96
S3 1412 x 1200	Four point	45° (r=0.85)	17.40	14.50	0.83	69.00	67.00	0.97
S4 1412 x 1200	Four point	25° (r=0.85)	19.20	16.40	0.85	75.00	73.50	0.98
S5 800 x 1200	One point	25° (r=1.50)	9.10	7.25	0.80	50.50	52.00	1.03
S6 800 x 1200	Four point	25° (r=1.50)	11.00	9.25	0.84	51.50	53.50	1.04

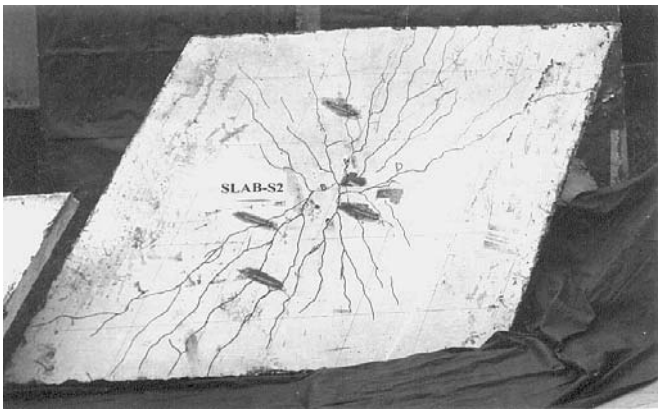

Fig. 8. Cracks at failure on the tension side of the test Slab S2 (Single point load)

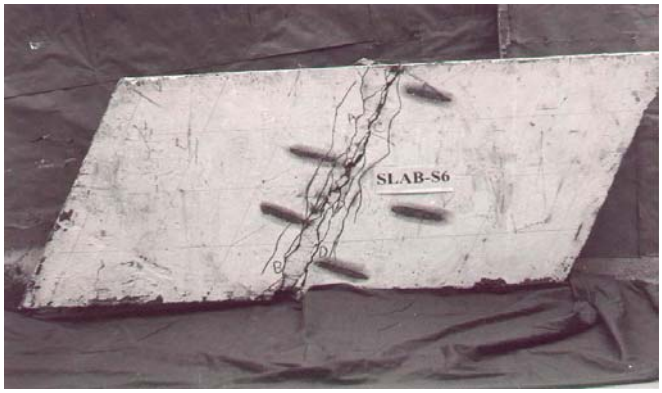

Fig. 9. Cracks at failure on the tension side of the test Slab S2 (Four point line loads)

6. Conclusions

The following conclusions may be drawn based on the observations of the present experimental study:

(i) The load carrying capacity of skew slabs significantly depends on the skew angle. As can be expected, with the increase in skew angle stiffness of slab decrease and so is load carrying capacity.

(ii) For the same aspect ratio and skew angle, the ultimate (total) load carrying capacity of skew slabs are higher in case when the loads are distributed across the width like that of four point loads compared to a single point load at the central point.

(iii) The deflection at obtuse zone is more than acute zone in slabs with lower aspect ratio (r = 0.85) compared to slabs with higher aspect ratio (r = 1.50).

(iv) Cracks propagate toward free edges like a mesh crack and somewhat parallel to support line in case of a single concentrated load placed at the centre point.

(v) Cracks are limited within a small bandwidth parallel to support line along centre span for multiple point loads placed across the centre span.

(vi) Deflections of the central nodal point of the test slabs supporting single concentrated load are relatively higher than slabs supporting four point loads equal to that single load in magnitude.

(vii) Relatively wider cracks are formed in skew slabs supporting four points loading at center span compared to slabs loaded with single point load at central point.

(viii) Finite Element analysis using layered technique is found to be quite effective to estimate the ultimate load carrying capacity of the RC skew slabs.

References

AASHTO (1983). ″Standard Specification for Highway Bridges″ 13th edition, American Association of State Highway and Transportation Officials, Washington.

ASTM C 136 (1988). Test method for Sieve Analysis of Fine and Course Aggregates, Vol. 04.02, Section-4, American Society of Testing Materials, Philadelphia, pp. 76.

Cope, R. J. and Rao, P. V. (1983). Moment Redistribution in Skewed Slab Bridge, Proc. Instn. of Civil Engineers, Part 2, Vol. 75, September, pp. 419-451.

Desayi, P. and Probhakara, A. (1981). load Deflection Behaviour of Restrained R/C Skew Slabs, *Journal of the Structural Division ASCE*, 107, No. ST5, May, pp. 873 – 887.

Doullah, Sk. Md. Nizam-ud and Kabir A. (1997). Analysis of Reinforced Concrete Skew Slabs using Layered Mindlin Plate Element, *J. of Inst. of Engineers (India)*, 78, pp. 97-102, Nov.

Doullah, Sk. Md. Nizam-ud (2000). Nonlinear Finite Element Analysis of Reinforced Concrete Skew Slabs, Ph. D. Thesis, Department of Civil Engineering, BUET, Dhaka.

El-Hafez, L.M.A., (1986). Direct Design of Reinforced Concrete Skew Slabs, Ph.D. Thesis, University of Glasgow, UK.

Islam, N. M. (1996). Ultimate Load Behaviour of Skew Slab Bridge Deck, M. Sc. Engineering Thesis, Department of Civil Engineering, BUET, Dhaka.

Jahan, S. M. (1989). Investigation of Skew Slab Bridge, M. Sc. Engineering Thesis, Department of Civil Engineering, BUET, Dhaka.

Miah, M. K. (2000). Behaviour of Reinforced Concrete Skew Slab under Vertical Loads, M. Sc. Engineering Thesis, Department of Civil Engineering, BUET, Dhaka.

Zia, P., White, R. N. and Vanhorn, D. A. (1970). Principles of Model Analysis, ACI Special Publication SP-24, American Concrete Institute, Detroit, Michigan, pp. 19-39.